Comparative replication and immune activation profiles of SARS-CoV-2 and SARS-CoV in human lungs: an *ex vivo* study with implications for the pathogenesis of COVID-19

Hin Chu[1,a], Jasper Fuk-Woo Chan[1,2,3,4,a], Yixin Wang[1,a], Terrence Tsz-Tai Yuen[1,a], Yue Chai[1], Yuxin Hou[1], Huiping Shuai[1], Dong Yang[1], Binjie Hu[1], Xiner Huang[1], Xi Zhang[1], Jian-Piao Cai[1], Jie Zhou[1], Shuofeng Yuan[1], Kin-Hang Kok[1], Kelvin Kai-Wang To[1,2,3], Ivy Hau-Yee Chan[5], Anna Jinxia Zhang[1], Ko-Yung Sit[5], Wing-Kuk Au[5], Kwok-Yung Yuen[1,2,3,4]

[a]Co-first authors

[1]State Key Laboratory of Emerging Infectious Diseases, Carol Yu Centre for Infection, Department of Microbiology, Li Ka Shing Faculty of Medicine, The University of Hong Kong, Pokfulam, Hong Kong Special Administrative Region, China

[2]Department of Microbiology, Queen Mary Hospital, Pokfulam, Hong Kong Special Administrative Region, China

[3]Department of Clinical Microbiology and Infection Control, The University of Hong Kong-Shenzhen Hospital, Shenzhen, China

[4]Hainan Medical University-The University of Hong Kong Joint Laboratory of Tropical Infectious Diseases, Hainan Medical University, Haikou, Hainan, and The University of Hong Kong, Pokfulam, Hong Kong Special Administrative Region, China

[5]Department of Surgery, The University of Hong Kong, Queen Mary Hospital, Pokfulam, Hong Kong Special Administrative Region, China

Correspondence: Kwok-Yung Yuen (kyyuen@hku.hk). State Key Laboratory of Emerging Infectious Diseases, Carol Yu Centre for Infection, Department of Microbiology, Li Ka Shing Faculty of Medicine, The University of Hong Kong, Pokfulam, Hong Kong Special Administrative Region, China. Tel: 852-22552402. Fax: 852-28551241.

Summary:

The comparative viral kinetics, cell tropism, and innate immune response profiles of SARS-CoV-2 and SARS-CoV in human lungs were characterized in *ex-vivo* organ cultures. SARS-CoV-2 exhibited more efficient replication but induced significantly less host interferon and proinflammatory response than SARS-CoV.

ABSTRACT

Background. Severe acute respiratory syndrome coronavirus 2 (SARS-CoV-2) is an emerging coronavirus that has resulted in nearly 1,000,000 laboratory-confirmed cases including over 50,000 deaths. Although SARS-CoV-2 and SARS-CoV share a number of common clinical manifestations, SARS-CoV-2 appears to be highly efficient in person-to-person transmission and frequently cause asymptomatic infections. However, the underlying mechanism that confers these viral characteristics on high transmissibility and asymptomatic infection remain incompletely understood.

Methods. We comprehensively investigated the replication, cell tropism, and immune activation profile of SARS-CoV-2 infection in human lung tissues with SARS-CoV included as a comparison.

Results. SARS-CoV-2 infected and replicated in human lung tissues more efficiently than that of SARS-CoV. Within the 48-hour interval, SARS-CoV-2 generated 3.20 folds more infectious virus particles than that of SARS-CoV from the infected lung tissues ($P<0.024$). SARS-CoV-2 and SARS-CoV were similar in cell tropism, with both targeting types I and II pneumocytes, and alveolar macrophages. Importantly, despite the more efficient virus replication, SARS-CoV-2 did not significantly induce types I, II, or III interferons in the infected human lung tissues. In addition, while SARS-CoV infection upregulated the expression of 11 out of 13 (84.62%) representative pro-inflammatory cytokines/chemokines, SARS-CoV-2 infection only upregulated 5 of these 13 (38.46%) key inflammatory mediators despite replicating more efficiently.

Conclusions. Our study provided the first quantitative data on the comparative replication capacity and immune activation profile of SARS-CoV-2 and SARS-CoV infection in human lung tissues. Our results provided important insights on the pathogenesis, high transmissibility, and asymptomatic infection of SARS-CoV-2.

Keywords. coronavirus; COVID-19; *ex vivo*; interferon; SARS-CoV-2.

The novel Coronavirus Disease 2019 (COVID-19) pandemic caused by the severe acute respiratory syndrome coronavirus 2 (SARS-CoV-2) has affected nearly 1,000,000 patients with over 50,000 deaths within 3 months, whereas the 2002-2003 SARS caused by SARS-CoV was controlled within 6 months and only affected 8,096 patients with 774 deaths.[1,2] The genome of SARS-CoV-2 was most homologous to Chinese horseshoe bat SARS-related coronaviruses and was speculated to have jumped into a yet unknown wild animal being traded in a Wuhan wet market in China where this pandemic agent was first detected in the environmental samples.[2,3] Apparently more efficient person-to-person transmission than 2003 SARS was soon noticed in the settings of family, church, community, cruise ship, nursing home, and hospital.[4-8] Despite the much lower crude fatality rate of COVID-19 (0.25% to 5%) than that of SARS (about 10%), the high number of patients affected in this ongoing pandemic due to a complete lack of population herd immunity resulted in a staggering number of deaths.[9] The clinical manifestations of COVID-19 can vary from asymptomatic virus shedding among household contacts, mild upper respiratory tract infection, acute asymptomatic walking pneumonia, to symptomatic pneumonia with bilateral multifocal ground-glass opacities on lung imaging studies, and severe pneumonia with acute respiratory distress syndrome and multiorgan failure.[10] Though animal models of non-human primate, human angiotensin-converting enzyme 2 (ACE2) transgenic mouse, and golden Syrian hamster successfully challenged by SARS-CoV-2 have recently been reported, studies on the pathogenesis of COVID-19 in human subjects are still largely lacking.[11-13] While bronchoalveolar lavage was frequently performed in severe COVID-19 patients for making a virological diagnosis, transbronchial or open lung biopsy for detecting the histopathological changes and host response in the human lung induced by SARS-CoV-2 was almost never performed for understanding the pathogenesis in these severe patients with respiratory failure. Post-mortem examinations were also rarely performed until multi-organ failure developed

after weeks of intensive care by intubation and ventilation.[14] In this study, we used *ex vivo* human lung tissue challenged by SARS-CoV-2 with SARS-CoV as control to quantitatively characterise the viral kinetics, cell type tropism, virus protein expression, and host cytokine/chemokine responses. It is notable that the *ex vivo* lung tissue from each individual donor patient can be divided into two parts for parallel challenge by the test SARS-CoV-2 and the control SARS-CoV. Thus this *ex vivo* lung model system provides a unique opportunity for side by side comparison of the virological and host response characteristics that clinical studies on patients or animal models cannot achieve. The findings are important in understanding the relatively more efficient transmissibility of COVID-19 and the innate immune mechanism behind this phenomenon.

METHODS

Viruses and biosafety

SARS-CoV-2 HKU-001a (GenBank accession number MT230904) was isolated from the nasopharyngeal aspirate of a laboratory-confirmed COVID-19 patient in Hong Kong as previously described.[15] SARS-CoV GZ50 (GenBank accession number AY304495) was an archived clinical isolate at Department of Microbiology, HKU. Both SARS-CoV-2 and SARS-CoV were propagated and titered in VeroE6 cells with plaque assays as previously described.[15,16] All experiments involving infectious SARS-CoV-2 and SARS-CoV followed the approved standard operating procedures of our Biosafety Level 3 facility at the Department of Microbiology, HKU.

Human *ex vivo* lung tissues

Human lung tissues for *ex vivo* studies were obtained from patients undergoing surgical operations at Queen Mary Hospital, Hong Kong as we previously described.[17] All donors gave written consent as approved by the Institutional Review Board of the University of Hong Kong/Hospital Authority Hong Kong West Cluster (UW13-364). The freshly obtained lung tissues were processed into small rectangular pieces and were rinsed with advanced Dulbecco's Modified Eagle's Medium (DMEM)/F12 medium (Gibco, Thermo Fisher Scientific, Waltham, MA, USA) supplemented with 2mM of 4-(2-hydroxyethyl)-1-piperazineethanesulfonic acid (HEPES) (Gibco), 1×GlutaMAX (Gibco), 100U/ml penicillin, and 100μg/ml streptomycin. The specimens were infected with SARS-CoV-2 or SARS-CoV with an inoculum of 1×10^6PFU/ml at 500μl per well. After 2h, the inoculum was removed and the specimens were washed with phosphate-buffered saline (PBS) 3 times. The infected human lung tissues were then cultured in 1.2ml of advanced DMEM/F12 medium with 2mM HEPES (Gibco), 1×GlutaMAX (Gibco), 100U/ml penicillin, 100μg/ml streptomycin, 20μg/ml vancomycin, 20μg/ml ciprofloxacin, 50μg/ml amikacin, and 50μg/ml nystatin. Supernatants were collected at 2, 24, and 48 hours post-inoculation (hpi) for plaque assays. The lung tissues were harvested at 2, 24, and 48hpi in RL buffer (Qiagen, Hilden, Germany) with DTT (Qiagen) for quantitative reverse transcription-polymerase chain reaction (qRT-PCR) analysis or fixed in 10% formalin for immunostaining and immunohistochemistry studies.

Immunofluorescence staining and confocal microscopy

Immunofluorescence staining and confocal microscopy were performed as previously described with slight modifications.[15,18,19] Briefly, infected human lung tissue samples were harvested and fixed overnight using 10% formalin, and then processed with a TP1020 Leica

semi-enclosed benchtop tissue processor with serially increasing concentration of ethanol, xylene, and wax for 16h, before being embedded in wax. Formalin-fixed, paraffin-embedded human lung tissues were then sectioned at 4μm with a Thermo Fisher Scientific HM 355S rotary microtome. Tissue sections were fished and dried to fix on Thermo Fisher Scientific Superfrost Plus slides at 37°C overnight before deparaffinising and immunofluorescence staining. Serially increasing concentrations of xylene and ethanol were applied for dewaxing. In order to expose the viral nucleocapsid (N) antigens, the slides were heated with antigen unmasking solution (Vector Laboratories, Burlingame, CA, USA) in a pressure cooker for 90s. After blocking with serum-free protein block and Sudan black B, the slides were stained with an in-house mouse anti-SARS-CoV-2-N immune serum or an in-house mouse anti-SARS-CoV-N immune serum. The secondary antibody goat anti-mouse IgG H&L (Alexa Fluor® 488) was obtained from Thermo Fisher Scientific. Mounting was performed with the antifade mounting medium with DAPI (Vector Laboratories). Images were acquired with confocal microscopy using a ZEISS LSM710 system with the 20×objective as previously described.[20] Image fields were selected and processed with the ZEN software blue edition (ZEISS) at the resolution of 1024×1024 pixels. To quantify the relative fluorescence intensity, multiple images from infected human lung tissues of two representative donors were split into separate channels and the intensity of channel 488 nm was quantified with ImageJ.

Histology and immunohistochemistry staining

Histology and immunohistochemistry staining were performed as previously described with slight modifications.[13] Briefly, fixed human tissues were processed, embedded, and cut to prepare 4μm tissue sections on glass slides. Slides were dewaxed with xylene and serially decreased concentrations of ethanol before staining. To detect SARS-CoV-2-N and SARS-

CoV-N antigens, tissue sections underwent the same antigen retrieval procedures as those of immunofluorescence staining, followed by blocking with 0.3% hydrogen peroxide for 30min to abolish the activity of any potential endogenous peroxidase. The slides were subsequently incubated with an in-house mouse anti-SARS-CoV-2-N immune serum or an in-house mouse anti-SARS-CoV-N immune serum, and then incubated with Mouse-on-Mouse Polymer (Abcam, Cambridge, UK). The signal was developed with the DAB (3,3'-diaminobenzidine) substrate kit (Vector Laboratories). The nuclei were developed with Gill's haematoxylin before mounting the slides with VectaMount permanent mounting medium (Vector Laboratories). Images were acquired with the Olympus BX53 light microscope using 40×objective.

Plaque assays

VeroE6 cells were maintained in DMEM with 10% FBS, 1% penicillin, and 1% streptomycin. The cells were seeded one day before the experiment at 2×10^5 cells per well in 12-well plates and were allowed to grow at 37°C overnight. For the plaque assay, serially diluted samples were inoculated on the cells for 1h. Afterwards, 3% agarose/PBS was mixed with DMEM with 1.5% fetal bovine serum at a 1:2 ratio and applied to the cells. The cells were incubated for 96h for plaque formation. The plaques were visualized by staining the plates with 1% crystal violet in 20% ethanol/distilled water for 15min.

RNA extraction and qRT-PCR

Cell lysate samples from the infected lung tissues were harvested at 2, 24, and 48hpi for qRT-PCR detection of mRNA levels of interferon (IFN) and cytokine/chemokine markers. Briefly, lung tissues were homogenised and lysed with RL buffer for RNA extraction using the RNeasy Mini kit (Qiagen). qRT-PCR was then performed using the QuantiNova SYBR

Green RT-PCR kit (Qiagen) with LightCycler 480 Real-Time PCR System (Roche, Basel, Switzerland) to quantify the expression level of different host markers. Each 20μl reaction mixture contained 10μl of 2×QuantiNova SYBR Green RT PCR Master Mix, 2.6μl of RNase-free water, 0.2μl of QuantiNova SYBR Green RT-Mix, 1.6μl each of 10μM gene-specific forward and reverse primer, and 4μl of extracted RNA as template. Reactions were incubated at 45°C for 10min for reverse transcription, 95°C for 5min for denaturation, followed by 45 cycles of 95°C for 5s and 55°C for 30s. Signal detection and measurement were taken in each cycle after the annealing step. The cycling profile ended with a cooling step at 40°C for 30s. The primer sequences are available upon requested.

Statistical analysis

Statistical analyses for the quantification of viral N antigen expression from SARS-CoV-2- or SARS-CoV-infected human lung tissues were performed with one-way ANOVA using GraphPad Prism 6 (GraphPad Software, Inc.). Statistical analyses for the area under the curve (AUC) comparison between SARS-CoV-2- and SARS-CoV-generated infectious virus particles from the infected human lung tissues were performed with Student's t-test using GraphPad Prism 6 as previously described.[15] Statistical analyses for SARS-CoV-2- or SARS-CoV-induced cytokine/chemokine expressions were performed with two-way ANOVA using GraphPad Prism 6. Differences were considered statistically significant when $P<0.05$.

RESULTS

Comparative infection and replication capacity of SARS-CoV-2 and SARS-CoV in *ex vivo* human lung tissue explants

A total of six patient donors were included in this study. These included 3 females and 3 males with a mean age of 53 years (range, 47-64 years) who underwent wedge resection or lobectomy for lung tumour. To evaluate their differential capacities to infect and replicate in human lung tissue, we inoculated human lung tissue explants with SARS-CoV-2 or SARS-CoV with an inoculum of 1×10^6 plaque-forming units per ml (PFU/ml) at 500µl per well. The infected samples were harvested at 24hpi and examined for viral N antigen expression. With immunostaining and confocal microscopy, we demonstrated that both SARS-CoV-2 and SARS-CoV could infect human lung tissues as evidenced by viral N antigen expression in representative images of two donors (Figure 1). Intriguingly, SARS-CoV-2-N antigens were consistently detected in higher abundance and in broader areas of the lung tissues of all donors than that of SARS-CoV-N antigens (Figure 1). Quantitative analysis confirmed that the relative fluorescent intensity of SARS-CoV-2-N antigen was significantly ($P<0.0001$ to 0.041) higher (2.30 to 2.87 folds) than SARS-CoV-N antigen in the donors' lung tissues (Supplementary Figure 1). To more thoroughly quantify the different infectiveness and replication of the two viruses in human lung tissues, we inoculated additional lung tissue samples and measured the infectious virus titers generated at 2, 24, and 48hpi with plaque assays. Among the four lung tissues evaluated, the maximum SARS-CoV-2 titer increased between 2hpi and 48hpi ranged from 1.20logs to 2.04logs. With the same experimental setting, the maximum SARS-CoV titer increase between 2hpi and 48hpi ranged from 0.61log to 1.15logs only (Figure 2A). To determine the relative replicaiton capacity of the two viruses in lung tissues, we set the virus titer at 2hpi as the baseline, which represented the residual inoculum after inoculation and wash, and calculated the virus titer increase from the baseline

at 24hpi and 48hpi. As shown in Figure 2B, SARS-CoV-2 consistently demonstrated higher virus titer increases than that of SARS-CoV in lung tissues from all four donors. Our area under the curve (AUC) analysis revealed that SARS-CoV-2 generated 3.20 folds more infectious virus particles than that of SARS-CoV from the infected lung tissues over a period of 48h ($P<0.024$) (Figure 2C). Taken together, our results illustrated that SARS-CoV-2 was capable of infecting and replicating more robustly than SARS-CoV in human lung tissues.

Cell tropism of SARS-CoV-2 and SARS-CoV in human lung tissues

To identify the cell types targeted by SARS-CoV-2 and SARS-CoV in the human lung, we performed immunohistochemistry staining of the virus-infected lung tissues (Figures 3A to 3N). Our results clearly demonstrated that SARS-CoV-2 could infect type I pneumocytes (Figures 3A to 3C), type II pneumocytes (Figures 3E to 3H), as well as alveolar macrophages (Figure 3D). In this regard, the cell tropism of SARS-CoV-2 in the human lung was similar to that of SARS-CoV, which also targeted types I and II pneumocytes (Figures 3I to 3J) and alveolar macrophages (Figure 3K to 3L).

Expression profiles of interferons and pro-inflammatory mediators in SARS-CoV-2- and SARS-CoV-infected human lung tissues

Next, to assess the innate immune responses induced by SARS-CoV-2 and SARS-CoV in human lung tissues, we investigated the expression of a panel of representative interferons (IFNs) and pro-inflammatory cytokines/chemokines upon virus challenge. Our data demonstrated that the 2003 SARS-CoV infection resulted in significant upregulation of types I (IFNβ), II (IFNγ), and III (IFNλ1, IFNλ2, and IFNλ3) IFNs in human lung tissues. In contrast, SARS-CoV-2 infection did not significantly trigger the expression of any IFN at all evaluated time points (Figure 4). In addition to types I, II, and III IFNs, we evaluated the

expression of four key pro-inflammatory cytokines (Figure 5A) and nine key pro-inflammatory chemokines (Figure 5B) that have critical roles in immune cell recruitment and activation. Our data showed that SARS-CoV infection resulted in significant activation of 11 out of 13 (84.62%) evaluated pro-inflammatory factors at either 24hpi or 48hpi. In contrast, SARS-CoV-2 infection only significantly upregulated five of these 13 (38.46%) inflammatory mediators including IL6, MCP1, CXCL1, CXCL5, and CXLC10 (IP10). In addition, among all assessed IFNs and cytokines/chemokines, the expression of 12 out of 19 (63.16%) genes were significantly lower in SARS-CoV-2-infected human lung tissues in comparison to that of the SARS-CoV-infected samples (Figures 4 and 5). Only IP10 was significantly more induced by SARS-CoV-2 than SARS-CoV. Collectively, our results illustrated that SARS-CoV-2 generally triggered significantly lower levels of IFNs and pro-inflammatory cytokines/chemokines despite being capable of infecting and replicating in the human lung at significantly higher efficiency.

DISCUSSION

Using *ex vivo* human lung tissue explants respectively challenged by the same inoculum of SARS-CoV-2 and SARS-CoV, we showed that SARS-CoV-2 was more capable than SARS-CoV in infecting and replicating in human lung tissues. While both viruses infected type I and type II pneumocytes, and alveolar macrophages as target cells, the amount of viral N antigen expression in the virus-challenged lung tissues was significantly higher and more intensive in the tissues infected with SARS-CoV-2 than those infected with SARS-CoV. Moreover, SARS-CoV-2 produced 3.20 folds higher amounts of infectious virus particles than that of SARS-CoV within 48 hpi. These findings might explain the high viral load in the respiratory secretions of COVID-19 patients during the early days on presentation or even during incubation, and thus its high person-to-person transmissibility.[4,21] Importantly, we

demonstrated that SARS-CoV-2 triggered lower levels of IFNs and pro-inflammatory cytokines/chemokines despite being capable of infecting and producing significantly higher amount of virus in human lung tissues. While the innate immune response in infected cells is our first line of defence against acute viral infection, SARS-CoV-2 infection did not significantly trigger any IFN response at all, and only significantly activated 5 of 13 pro-inflammatory mediators. Thus, unlike SARS patients who generally presented with high fever followed by rapidly progressive pneumonia and then respiratory failure with a mortality rate of about 10%, only about 16% of COVID-19 patients are severely ill and less than 5% percent of them died.[2,10] The low degree of innate immune activation could also account for the mild or even lack of symptoms in many COVID-19 patients who were not even tested and unknowingly spreading the virus in both community and hospital settings, making the pandemic control much more difficult than SARS.

While both 2019 SARS-CoV-2 and 2003 SARS-CoV can attach and enter host cells via ACE2, the mechanism of how SARS-CoV-2 overcome the innate immune response and suppress the IFN and proinflammatory cytokines and chemokines to achieve a higher degree of viral replication is still elusive. Despite that the N protein of both of these coronaviruses share 94% of amino acid similarity[3], significantly higher N expression in terms of both the extent and intensity was readily observed in SARS-CoV-2-infected *ex vivo* lung tissues. Studies of SARS-CoV in cell culture suggested that its N protein antagonized IFNβ response in a dose-dependent manner.[22] Moreover, two other SARS-CoV proteins, namely Orf3b and Orf6, also antagonise IFN synthesis and signalling pathway.[23] While SARS-CoV-2 is also postulated to possess IFN antagonising proteins, the exact identities of these proteins remain undetermined at this stage. The differential degrees of IFN inhibition by these viruses' IFN antagonising proteins may explain the discrepant viral replications and inflammatory responses in human lungs observed in the present study. Moreover, most proinflammatory

cytokines and chemokines except IP10, a chemoattractant for monocytes/macrophages, T cells and NK cells, were more significantly induced by SARS-CoV than SARS-CoV-2. This finding may explain the more severe disease and higher mortality of SARS than that of COVID-19.

In contrast to SARS patients who had rising viral load in nasopharyngeal secretions that peaked at around day 10, the viral load in the respiratory secretions of COVID-19 patients peaked much earlier at the time of symptom onset.[21,24]. The viral kinetics and innate immune response profiles in *ex vivo* human lung tissue characterised in this study might help to explain this observation. The suboptimally activated innate immune response would allow SARS-CoV-2 to replicate to high levels in the respiratory tract early on and may contribute to its efficient person-to-person transmission via droplets or contact with contaminated respiratory secretions containing high viral loads.[4,21,25] Notably, the higher degree of viral infection and replication of SARS-CoV-2 in human lung tissues corroborated with our recent finding that SARS-CoV-2 exhibited more efficient replication in Calu3 (human lung adenocarcinoma) cells than SARS-CoV.[15]

Our findings have important implications on the infection control and treatment strategies for COVID-19 as SARS-CoV-2-infected patients may be infectious during the incubation period before onset of clinical symptoms due to its efficient suppression of host innate immune and proinflammatory response as evidenced by our findings.[26] Thus, in addition to hand washing and social distancing, universal masking was recommended in East Asia as a key epidemiological control measure to prevent virus shedding from subclinical patient sources and to prevent infection of susceptible individuals in the community.[27] Similar to influenza which is the most well studied acute respiratory virus infection, the viral load in the respiratory secretions of COVID-19 patients also peaks at the time of symptom onset, antiviral treatment for COVID-19 may not be very effective if given later than 48

hours after symptom onset. Thus, unlike SARS and Middle East respiratory syndrome which have viral loads peaking at day 7 to day 10 and therefore sufficient time for antivirals to act and reduce the peak viral loads, early initiation of antiviral therapy would be even more important to improve the clinical outcome of COVID-19.[24,28] Moreover, the use of high-dose corticosteroids and antagonists against major inflammatory mediators such as interleukin 6 should only be used together with effective antivirals to avoid over-suppression of the innate immune response in COVID-19 patients as SARS-CoV-2 is already suppressing the host innate immune response at the beginning of the infection.[29]

There were limitations in this study. First, the *ex vivo* human lung tissue explant culture is short-lasting and cannot represent the effect of host systemic inflammatory response and the adaptive immune response. Second, the supply of human lung tissues is limited and thus it was not possible for us to investigate the characteristics of different SARS-CoV-2 strains in this *ex vivo* model. More studies should be performed using both *ex vivo* lung and intestinal organoids to elucidate additional details on the pathogenesis of SARS-CoV-2 during pulmonary and extrapulmonary involvement.

Notes

Author contributions. HC, JF-WC, and K-YY had roles in the study design, data collection, data analysis, data interpretation, and writing of the manuscript. YW, TT-YY, YC, YH, HS, DY, BH, XH, XZ, J-PC, JZ, SY, K-HK, KK-WT, IH-YC, AJZ, K-YS, TW-KA had roles in the experiments, data collection, data analysis, and data interpretation. All authors reviewed and approved the final version of the manuscript.

Acknowledgements. This study was partly supported by the donations of May Tam Mak Mei Yin, Richard Yu and Carol Yu, the Shaw Foundation of Hong Kong, Michael Seak-Kan Tong, Respiratory Viral Research Foundation Limited, Hui Ming, Hui Hoy and Chow Sin Lan Charity Fund Limited, Chan Yin Chuen Memorial Charitable Foundation, Marina Man-Wai Lee, the Hong Kong Hainan Commercial Association South China Microbiology Research Fund, the Jessie & George Ho Charitable Foundation, and Perfect Shape Medical Limited; and funding from the Consultancy Service for Enhancing Laboratory Surveillance of Emerging Infectious Diseases and Research Capability on Antimicrobial Resistance for Department of Health of the Hong Kong Special Administrative Region Government; the Theme-Based Research Scheme (T11/707/15) of the Research Grants Council; Hong Kong Special Administrative Region; Sanming Project of Medicine in Shenzhen, China (No. SZSM201911014); and the High Level-Hospital Program, Health Commission of Guangdong Province, China. The funding sources had no role in the study design, data collection, analysis, interpretation, or writing of the report.

Potential conflicts of interest. We declare no competing interests.

REFERENCES

1. Cheng VC, Lau SK, Woo PC, Yuen KY. Severe acute respiratory syndrome coronavirus as an agent of emerging and reemerging infection. *Clin Microbiol Rev* 2007; **20**(4): 660-94.
2. World Health Organization. Coronavirus disease (COVID-19) Situation Report - 74. 3 April 2020. https://www.who.int/docs/default-source/coronaviruse/situation-reports/20200403-sitrep-74-covid-19-mp.pdf?sfvrsn=4e043d03_4 (accessed 4 April 2020).
3. Chan JF, Kok KH, Zhu Z, et al. Genomic characterization of the 2019 novel human-pathogenic coronavirus isolated from a patient with atypical pneumonia after visiting Wuhan. *Emerg Microbes Infect* 2020; **9**(1): 221-36.
4. Chan JF, Yuan S, Kok KH, et al. A familial cluster of pneumonia associated with the 2019 novel coronavirus indicating person-to-person transmission: a study of a family cluster. *Lancet* 2020.
5. Cheng VCC, Wong SC, Chen JHK, et al. Escalating infection control response to the rapidly evolving epidemiology of the Coronavirus disease 2019 (COVID-19) due to SARS-CoV-2 in Hong Kong. *Infect Control Hosp Epidemiol* 2020: 1-24.
6. Rocklov J, Sjodin H, Wilder-Smith A. COVID-19 outbreak on the Diamond Princess cruise ship: estimating the epidemic potential and effectiveness of public health countermeasures. *J Travel Med* 2020.
7. McMichael TM, Currie DW, Clark S, et al. Epidemiology of Covid-19 in a Long-Term Care Facility in King County, Washington. *N Engl J Med* 2020.
8. Pung R, Chiew CJ, Young BE, et al. Investigation of three clusters of COVID-19 in Singapore: implications for surveillance and response measures. *Lancet* 2020; **395**(10229): 1039-46.

9. Wilson N, Kvalsvig A, Barnard LT, Baker MG. Case-Fatality Risk Estimates for COVID-19 Calculated by Using a Lag Time for Fatality. *Emerg Infect Dis* 2020; **26**(6).

10. Guan WJ, Ni ZY, Hu Y, et al. Clinical Characteristics of Coronavirus Disease 2019 in China. *N Engl J Med* 2020.

11. Bao L, Deng W, Gao H, et al. Reinfection could not occur in SARS-CoV-2 infected rhesus macaques. 2020.

12. Bao L, Deng W, Huang B, et al. The Pathogenicity of SARS-CoV-2 in hACE2 Transgenic Mice. 2020.

13. Chan JF, Zhang AJ, Yuan S, et al. Simulation of the clinical and pathological manifestations of Coronavirus Disease 2019 (COVID-19) in golden Syrian hamster model: implications for disease pathogenesis and transmissibility. *Clin Infect Dis* 2020.

14. Tian S, Hu W, Niu L, Liu H, Xu H, Xiao SY. Pulmonary Pathology of Early-Phase 2019 Novel Coronavirus (COVID-19) Pneumonia in Two Patients With Lung Cancer. *J Thorac Oncol* 2020.

15. Chu H, Chan JF, Yuen TT, et al. An observational study on the comparative tropism, replication kinetics, and cell damage profiling of SARS-CoV-2 and SARS-CoV: implications for clinical manifestations, transmissibility, and laboratory studies of COVID-19. *Lancet Microbe* 2020.

16. Chan JF, Yip CC, To KK, et al. Improved molecular diagnosis of COVID-19 by the novel, highly sensitive and specific COVID-19-RdRp/Hel real-time reverse transcription-polymerase chain reaction assay validated in vitro and with clinical specimens. *J Clin Microbiol* 2020.

17. Zhou J, Chu H, Li C, et al. Active replication of Middle East respiratory syndrome coronavirus and aberrant induction of inflammatory cytokines and chemokines in human macrophages: implications for pathogenesis. *J Infect Dis* 2014; **209**(9): 1331-42.

18. Chu H, Chan CM, Zhang X, et al. Middle East respiratory syndrome coronavirus and bat coronavirus HKU9 both can utilize GRP78 for attachment onto host cells. *J Biol Chem* 2018; **293**(30): 11709-26.

19. Chan CM, Chu H, Wang Y, et al. Carcinoembryonic Antigen-Related Cell Adhesion Molecule 5 Is an Important Surface Attachment Factor That Facilitates Entry of Middle East Respiratory Syndrome Coronavirus. *J Virol* 2016; **90**(20): 9114-27.

20. Chu H, Zhou J, Wong BH, et al. Middle East Respiratory Syndrome Coronavirus Efficiently Infects Human Primary T Lymphocytes and Activates the Extrinsic and Intrinsic Apoptosis Pathways. *J Infect Dis* 2016; **213**(6): 904-14.

21. To KK, Tsang OT, Leung WS, et al. Temporal profiles of viral load in posterior oropharyngeal saliva samples and serum antibody responses during infection by SARS-CoV-2: an observational cohort study. *Lancet Infect Dis* 2020.

22. Hu Y, Li W, Gao T, et al. The Severe Acute Respiratory Syndrome Coronavirus Nucleocapsid Inhibits Type I Interferon Production by Interfering with TRIM25-Mediated RIG-I Ubiquitination. *J Virol* 2017; **91**(8).

23. Kopecky-Bromberg SA, Martinez-Sobrido L, Frieman M, Baric RA, Palese P. Severe acute respiratory syndrome coronavirus open reading frame (ORF) 3b, ORF 6, and nucleocapsid proteins function as interferon antagonists. *J Virol* 2007; **81**(2): 548-57.

24. Peiris JS, Chu CM, Cheng VC, et al. Clinical progression and viral load in a community outbreak of coronavirus-associated SARS pneumonia: a prospective study. *Lancet* 2003; **361**(9371): 1767-72.

25. To KK, Tsang OT, Chik-Yan Yip C, et al. Consistent detection of 2019 novel coronavirus in saliva. *Clin Infect Dis* 2020.

26. Wei WE, Li Z, Chiew CJ, et al. Presymptomatic Transmission of SARS-CoV-2 — Singapore, January 23–March 16, 2020. *MMWR Morb Mortal Wkly Rep* 2020. doi: http://dx.doi.org/10.15585/mmwr.mm6914e1 [Epub ahead of print]

27. Chan KH, Yuen KY. COVID-19 epidemic: disentangling the re-emerging controversy about medical facemasks from an epidemiological perspective. *Int J Epidemiol* 2020 Mar 31. pii: dyaa044. doi: 10.1093/ije/dyaa044. [Epub ahead of print]

28. Chan JF, Lau SK, To KK, Cheng VC, Woo PC, Yuen KY. Middle East respiratory syndrome coronavirus: another zoonotic betacoronavirus causing SARS-like disease. *Clin Microbiol Rev* 2015; **28**(2): 465-522.

29. Xu X, Han M, Li T, et al. Effective Treatment of Severe COVID-19 Patients with Tocilizumab. http://chinaxiv.org/home.htm *ChinaXiv* 2020.

FIGURE LEGENDS

Figure 1. Confocal microscopy examination of SARS-CoV-2 and SARS-CoV replication in human lung tissues. Human lung tissues were challenged with SARS-CoV-2 or SARS-CoV with an inoculum of $1x10^6$ PFU/ml. At 24 hours post inoculation (hpi), the infected lung tissues were harvested, fixed in 10% formalin, and immunolabeled for viral antigen. SARS-CoV-2 nucleocapsid protein (N) was identified with an in-house mouse anti-SARS-CoV-2 N immune serum and SARS-CoV N was identified with an in-house mouse anti-SARS-CoV N immune serum. Representative images from two lung donors were shown. The experiment was repeated with another four donors with consistent findings. Bars represented 50 μm.

Figure 2. Comparative replication capacity of SARS-CoV-2 and SARS-CoV in human lung tissues. Human lung tissues from four independent donors were challenged with SARS-CoV-2 or SARS-CoV. Supernatant samples from the infected lung tissues were harvested at 2, 24, and 48 hpi. The virus titers were determined with plaque assays. (A) The virus titers of the four individual lung tissues were shown. (B) The amount of infectious virus particles increased over the 48-hours period upon SARS-CoV-2 or SARS-CoV inoculation was shown for each lung donor. (C) Area under the curve analysis of SARS-CoV-2- and SARS-CoV-infected human lung tissues demonstrated the total amount of live infectious virus particles generated over the 48-hours period. Results in (C) represented the mean and standard deviations from four independent donors from four independent experiments. Statistical significance in (C) was determined with Student's t-test. * indicated $P<0.05$.

Figure 3. Cell tropism of SARS-CoV-2 and SARS-CoV in human lung tissues. Human lung tissues were challenged with SARS-CoV-2 or SARS-CoV. At 24 hpi, the infected lung tissues were harvested, fixed in 10% formalin, and processed for immunohistochemistry examination of viral antigen. (A-H) SARS-CoV-2 N could be identified from type I pneumocytes (B and C), type II pneumocytes (C, F, and H), and alveolar macrophages (D). (I-K) SARS-CoV N could be identified from type I pneumocytes and type II pneumocytes (J) as well as alveolar macrophages (L). (M-N) Mock-infected human lung tissues processed and immunolabeled with the same set of antibodies did not show any specific signal. SARS-CoV-2 N was identified with an in-house mouse anti-SARS-CoV-2 N immune serum and SARS-CoV N was identified with an in-house mouse anti-SARS-CoV N immune serum. Blue arrows represented type I pneumocytes, orange arrows represented type II pneumocytes, and green arrows represented alveolar macrophages. The experiment was repeated with 3 donors with consistent findings. Bars represented 50 μm.

Figure 4. Interferon response of SARS-CoV-2- and SARS-CoV-infected human lung tissues. Human lung tissues were challenged with SARS-CoV-2 or SARS-CoV. At 2, 24, and 48 hpi, the infected lung tissues were harvested for qRT-PCR analysis of type I (IFNα and IFNβ), type II (IFNγ), and type III (IFNλ1, IFNλ2, and IFNλ3) interferons. The results represented values from four independent lung donors in four independent experiments, with three to five lung pieces per donor. Statistical significance was determined with two-way ANOVA. * indicated $P<0.05$, ** indicated $P<0.01$, *** indicated $P<0.001$.

Figure 5. Expression profile of pro-inflammaotry cytokines and chemokines from SARS-CoV-2- and SARS-CoV-infected human lung tissues. Human lung tissues were challenged with SARS-CoV-2 or SARS-CoV. At 2, 24, and 48 hpi, the infected lung tissues were harvested for qRT-PCR analysis of representative pro-inflammatory (A) cytokines and (B) chemokines. The results represented values from four independent lung donors in four independent experiments, with three to five lung pieces per donor. Statistical significance was determined with two-way ANOVA. * indicated P<0.05, ** indicated P<0.01, *** indicated P<0.001, **** indicated P<0.0001.

Figure 1

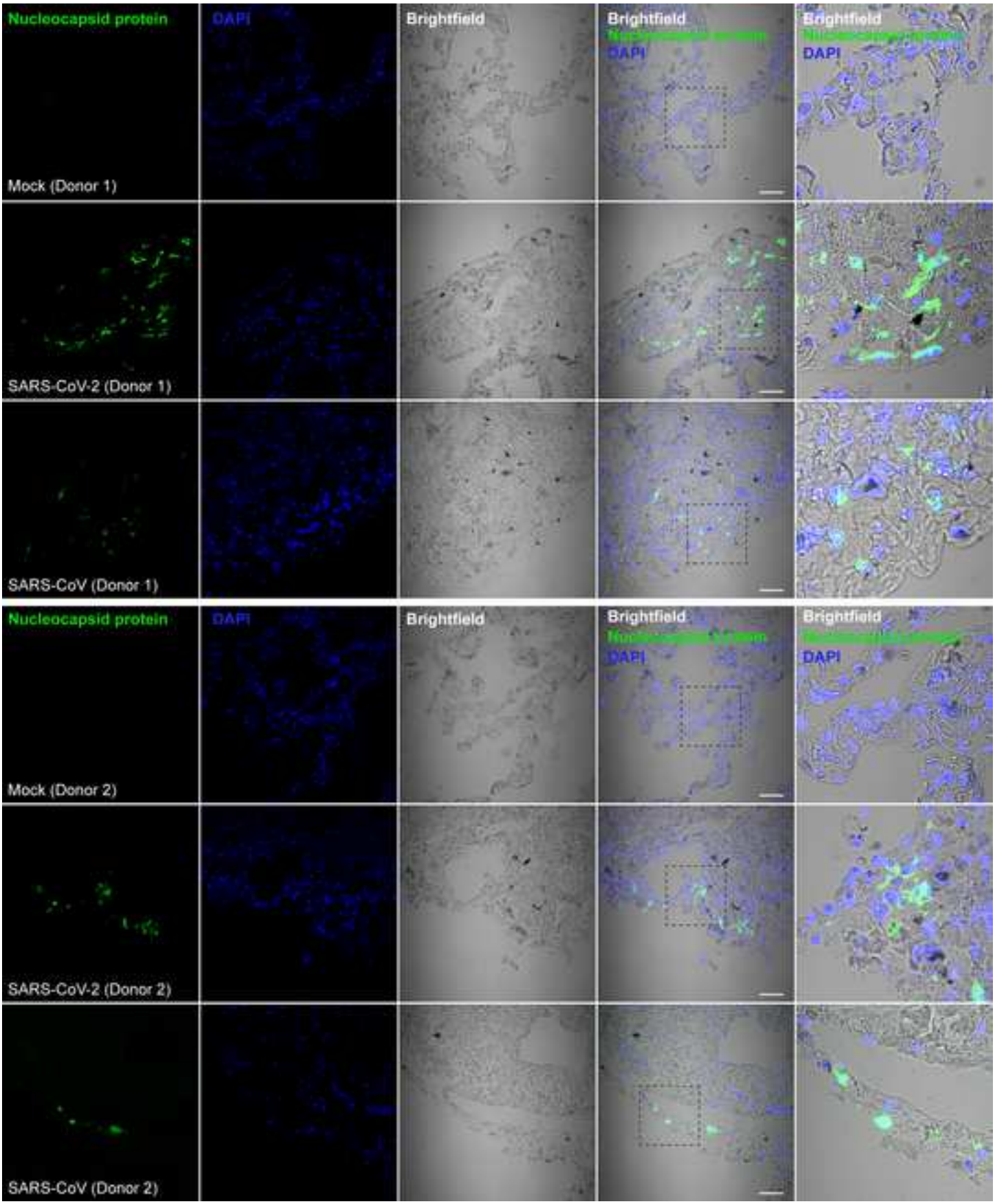

Figure 2

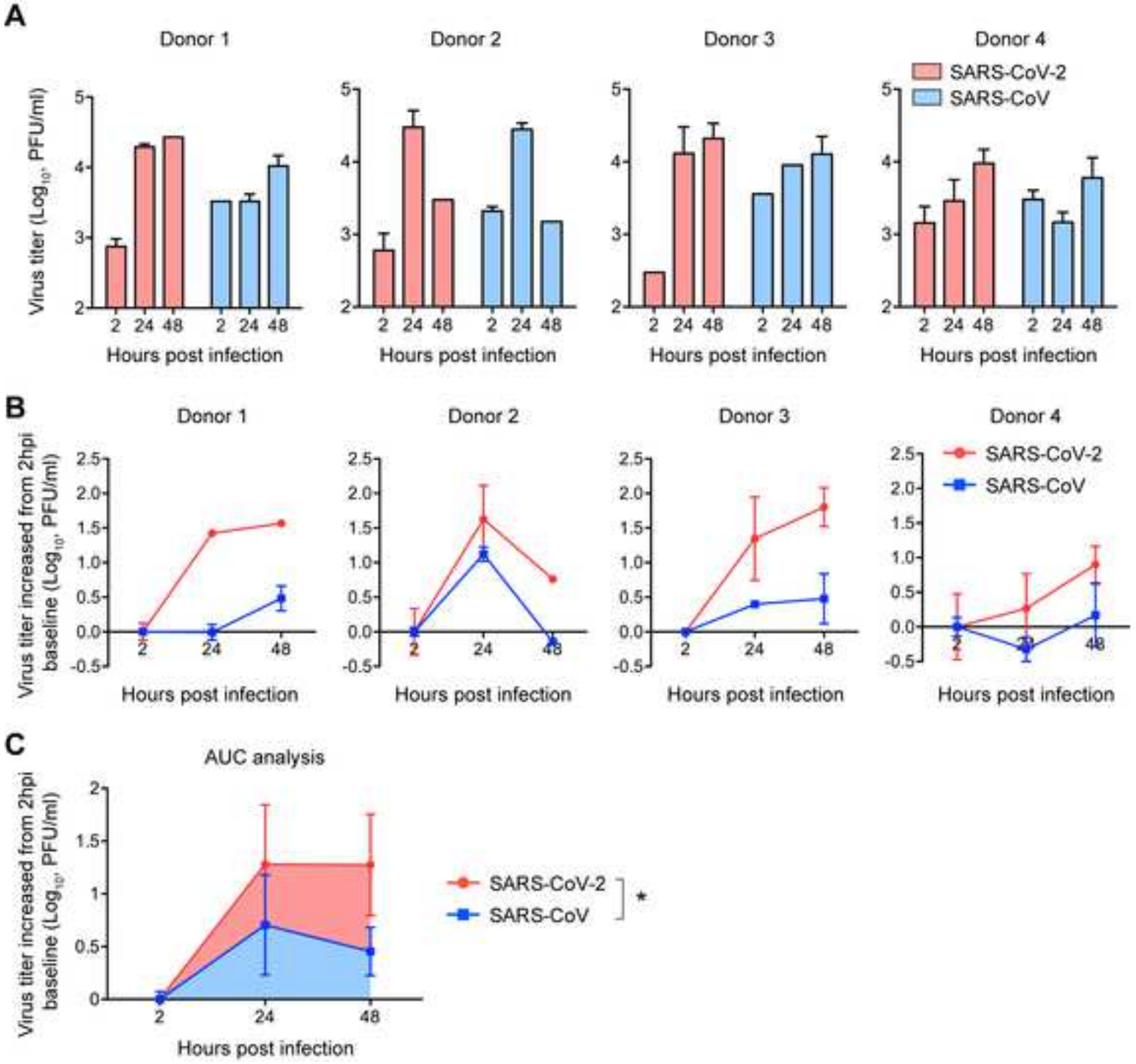

Figure 3

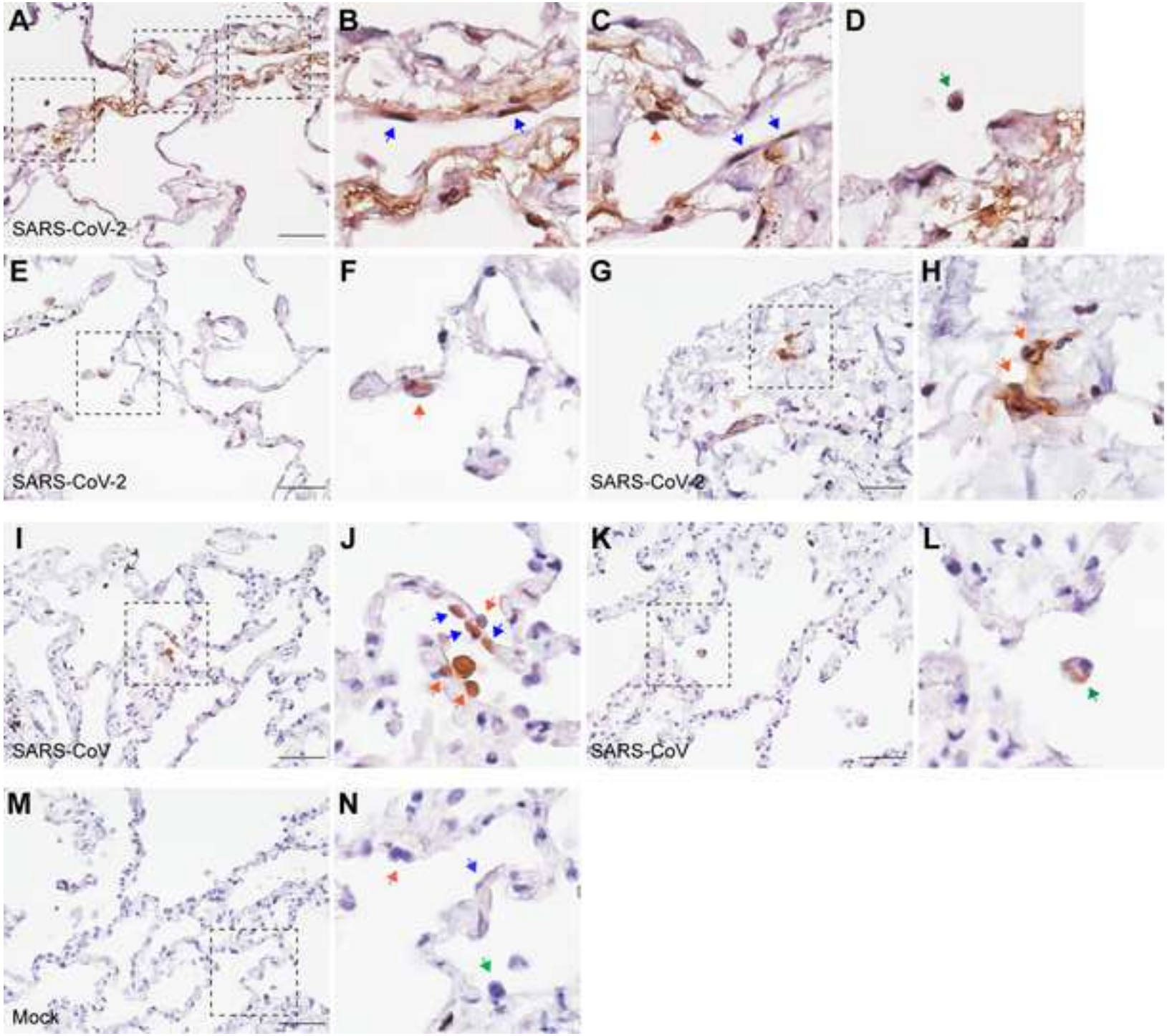

Figure 4

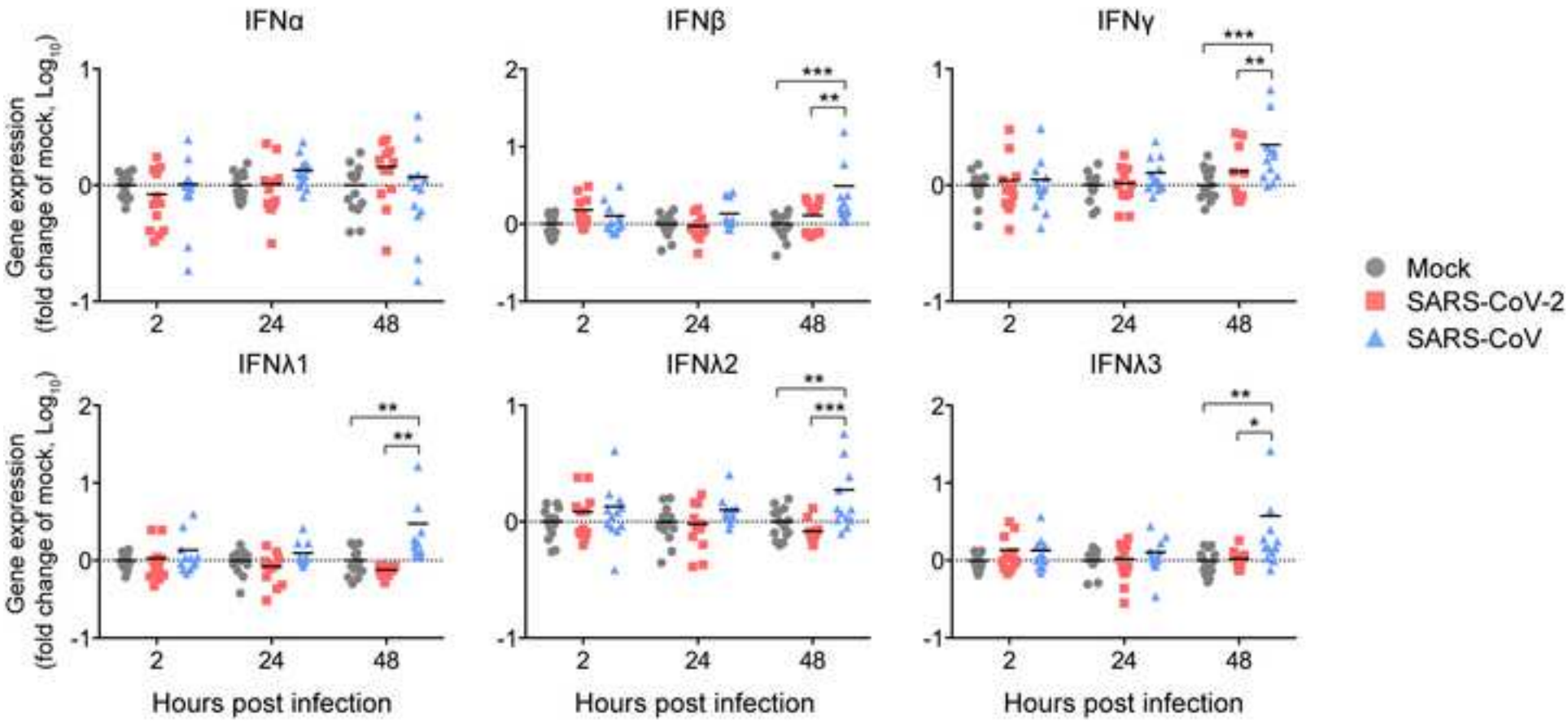

Figure 5